OPTIMIZATION-BASED FEEDFORWARD CONTROLLER DESIGN TO MINIMIZE THE EFFECTS OF CROSS-COUPLING OF A HELICOPTER WITH ARTICULATED-ROTOR

Oğuzhan Gültekin, Turkish Aerospace Industries (TAI), Ankara, Turkey
Can Ünen, Turkish Aerospace Industries (TAI), Ankara, Turkey
Umut Türe, Turkish Aerospace Industries (TAI), Ankara, Turkey
Ilgaz Doğa Okcu, Turkish Aerospace Industries (TAI), Ankara, Turkey

Abstract

In this study, TAI T-625 GÖKBEY helicopter pitch, roll and yaw axis cross coupling effects due to collective command and pitch axis cross coupling effects due to pedal command are minimized. A practical method, frequency domain magnitude curve minimization, is applied in frequency range of interest which is 0.3-20 rad/s. Mathematical model created by the flight mechanics team is used as the reference model to obtain off-axis response magnitude curves. A cost function, which defines difference between coupled and decoupled curves quantitatively, is used for minimization objective. The resultant controller is implemented to the helicopter. Flight tests are conducted to obtain time domain and frequency domain comparisons. In time domain comparisons, magnitudes of the responses are compared to verify decrement. For frequency domain comparisons, CIFER® tool is used and magnitude curves are compared to verify suppression in frequency range of interest and the results are found satisfactory.

1. NOTATION

Symbols:

q	Pitch rate, deg/s
p	Roll rate, deg/s
$\delta_{lon}, \delta_{lat}$	Pilot commands in pitch and poll axes, %
$\delta_{lon,AP}, \delta_{lat,AP}$	Autopilot commands in pitch and roll axes, %
H_{dcp}	Frequency response function with decoupling
$H_{no\ dcp}$	Frequency response function without decoupling

Acronyms:

AFCS	Automatic Flight Control System
SAS	Stability Augmentation System
ATT	Attitude Hold

2. INTRODUCTION

Helicopter flight dynamics is well known with its strong inter-axis couplings (Ref 1). In pilot point of view these couplings may be really disturbing, especially in precise tasks. Traditional linear control methods often ignore the nonlinear characteristics of helicopters and struggle to solve the strong coupling problem (Ref 2). In this study, a practical method to design feedforward decoupling controllers is suggested and applied to T-625 GÖKBEY helicopter. It's a 6-ton class multi-role helicopter that is equipped with a 4-axis limited authority AFCS with a SAS system for short-term rate damping and ATT for long-term angle stabilization.

Inter-axis couplings can be classified as control couplings and response couplings (Ref 3). Control couplings are the inter-axis relations due to given input and they arise with off-axis terms in the model's control derivatives. This type of couplings is directly excited by the given input and create an off-axis response. Response couplings are attributed to inertial, gyroscopic or aerodynamic effects and they show themselves in the model's stability derivatives. This type of couplings is not excited by the given input directly, instead they are excited by the on-axis response's itself. Helicopter dynamics includes both type of couplings.

For hover and forward flight helicopter inter-axis couplings are standardized in ADS-33E-PRF document (Ref 4). This standard document includes both time domain and frequency domain metrics for coupling investigations. The collective to yaw coupling in hover and collective to pitch coupling in forward flight are investigated in time domain metrics. In this study, a frequency domain decoupling design is proposed and shown that the time domain metrics are also improved significantly.

If the inter-axis coupling criteria outlined in ADS-33E-PRF are not met, a decoupling design technique must be implemented. One such technique is the dynamic cross-feed design, which has been successfully applied to UH-60 Black Hawk helicopters (Ref 5). However, this approach requires full authority fly-by-wire technology to be effective.

One approach to cross-coupling control in helicopters is the use of robust controllers. A robust controller is designed to handle uncertainties and disturbances in the system. It can effectively address the strong coupling problem in helicopters and improve their flight performance (Ref 6). Another approach is the use of adaptive control techniques. Adaptive control allows the controller to adjust its parameters based on the changing dynamics of the helicopter, enabling it to adapt to different flight conditions and effectively handle cross-coupling effects (Ref 7).

Goodwin et. al. proposes decoupling solutions for minimum phase or non-minimum phase stable plants and unstable plants (Ref 8). They classify the decoupled systems as dynamically decoupled systems, band decoupled (with statically decoupled) systems, triangularly coupled systems, and diagonally dominant systems. Dynamically decoupled systems represent completely diagonal systems while diagonally dominant systems have relatively small responses in off-diagonal elements of transfer function matrix. Band decoupled systems are diagonally dominant systems but only in a frequency range of interest. Triangularly coupled systems are beyond the scope of this study.

Parallel to the Goodwin's decoupling design for unstable plants, Liu Chen Hui addresses to Mezarovic's method (Ref 9). They both use stabilizing controllers before application of decoupling. Liu Chen Hui suggests a decentralized control as is used in GÖKBEY helicopters while Goodwin solves the problem with a multivariable feedback controller.

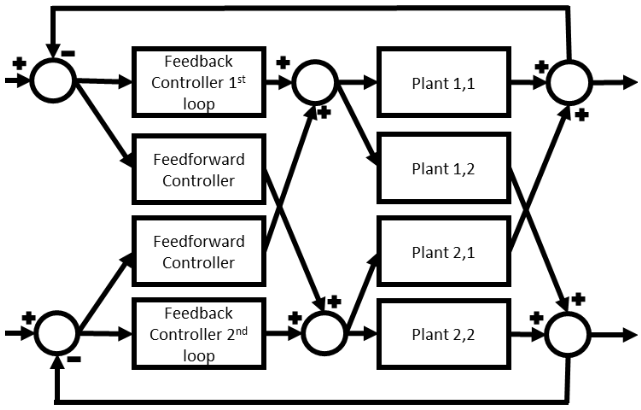

Figure 1. Mesarovic's idea in decoupling control architecture for 2 input 2 output system.

In this study Mesarovic's idea is followed with a practical method to design feedforward elements. The parameters of the feedforward controller were obtained through an optimization-based method, in which visual inspection techniques were frequently employed. It is important to note that mathematical optimization is rarely used by itself due to its impracticality, as some parameters require common use and therefore need to be selected based on user inspection. This situation is explained in section 3.3. Although artificial intelligence could potentially handle this selection in the future, the process is currently straightforward for the user. The objective of this work was to develop a practical method that avoids getting entangled in complex mathematical expressions, thus providing a distinctive approach that delivers results without becoming overwhelmed by theoretical intricacies.

3. Method

The design method used in this study will be based on feedforward controller design for frequency response function magnitude minimization in the frequency range of interest. Different input output relations can be considered to obtain these frequency domain minimizations. At first, two of these possible input-output relations and their pros and cons will be considered. After that, the decoupling architecture, the minimization process and the cost function will be explained. Those will be followed by decoupling designs. This will be for collective to yaw, pitch and roll couplings and pedal to pitch coupling since those are requested at first. However, the decoupling design procedure mentioned here is a general approach and may be expanded to any coupling in any system. At the end of the chapter general discussion will be held for the design procedure and a discussion will take place.

3.1. Input-Output Definition

Helicopter systems may have many inputs and many outputs based on their response types. T-625 helicopter is limited authority helicopter with inputs as $\delta_{lon}, \delta_{lat}, \delta_{ped}$ and δ_{coll}. Inter-axis couplings may be investigated from off-axis command to rate, angle or responsive autopilot actions as well as unit on-axis response to off-axis responses. The latter is the first candidate since this is well explained by Tischler et al. (Ref 3). Using these relations, the researchers aim to find the transfer function from on axis rate response to off axis rate responses. Since all rate responses are outputs in nature, this relation is defined by an inversion process. An example is frequency domain inter-axis coupling in the hover, pitch due to roll and roll due to pitch couplings. The rate relations are given as in the equations below:

For pitch due to roll **For roll due to pitch**

$$\frac{q}{p}(s) = \frac{\frac{q}{\delta_{lat}}}{\frac{p}{\delta_{lat}}} \qquad \frac{p}{q}(s) = \frac{\frac{p}{\delta_{lon}}}{\frac{q}{\delta_{lon}}}$$

Although this relation is also of interest in this study, command to command response relation is used more due to the lack of physical parameter effects in the former relation. Here, effects of the inertias can be an example for the physical parameter effect. For example, the helicopter pitch rate due to created unit roll rate could be equal to roll rate due to unit pitch rate, but the command required to compensate unit pitch rate is much higher than that for the unit roll rate because of the different body inertias in each axis. One can see that generated inputs' results in the body moments and this serves as a normalization process. Thus, comparability of the results is increased.

In pilot point of view the undesired response is pitch, roll and yaw responses to pilot collective command. To minimize these responses, one may also minimize the off-axis rate responses. However, rate responses introduce physical parameters effects, such as inertia that differs in between axes, which is undesired. Yet, the SAS mode is structured to generate commands by multiplying the rate responses with SAS gains. Hence, to be able to consider the off-axis responses, one can examine the off-axis autopilot responses in SAS mode. This way, one can compare the normalized results without any physical parameter effects. These transfer functions are given in the equations below:

For pitch due to roll **For roll due to pitch**

$$\frac{\delta_{lon,AP}}{\delta_{lat}}(s) \qquad \frac{\delta_{lat,AP}}{\delta_{lon}}(s)$$

Again, pitch due to roll and roll due to pitch couplings are considered here for illustration to keep the example and convention given by Tischler et al. The latter (rate to rate) and the former (pilot input to autopilot response) input-output relations are examined in this study and their results are shared in the upcoming sections.

3.2. Decoupling Architecture

The decoupling controller is decided to be implemented as a feedforward controller. Input of decoupling system is the pilot input and output of the system is the additive autopilot response in off-axes. For example, when the pilot applies collective input, the feedforward decoupling loop will create autopilot commands in pitch, roll and yaw axes to minimize responses in these axes. Further, an analysis will be done in frequency domain because a decoupling controller that is designed in time domain can have unexpectedly bad behavior in some frequencies that is not excited by the design input. The feedforward control loop is decided to include one high-pass and one low-pass filter with a DC gain. This structure can be used to construct a bandpass filter and the effective region that feedforward loop can suppress the off-axis response can be adjusted by filter cut-off frequencies. This has a crucial role, because this off-axis responses may have different dynamics in frequency range of interest. It will be shown in the design section that, half of the frequency range might be suppressed by using positive gains while the other half requires negative gains. In such situations, one may select the critical dynamics to suppress and adjust the effective region of the bandpass structure to decrease inverse effects on the other dynamics. Also, the high-pass filter is used to obtain the change in input size and obstruct actuator saturation. When the trim condition is obtained the input will have a dominant steady component which is filtered out by the high pass filter. After the input is applied in trim conditions, the high pass filter will permit the high frequency component of the input. The low-pass filter is also used to increase actuator lifetime, in addition to its bandpass action.

3.3. Minimization Process

Feedforward decoupling architecture is structured with one high pass filter, one lowpass filter and a DC gain. This requires optimization of three parameters. One may use optimization methods to obtain optimal values of those parameters, however finding constants for them is mostly useless because the helicopter flight envelope may have many different trim conditions and all of those trim conditions may require different high pass and lowpass filter cut-off frequencies. Switching or scheduling between those filter coefficients is not impractical and it is not proven to have a better response in between trim conditions. Thus, a design decision is made to have constant cut-off frequencies for filters and a scheduled gain. So, it is crucial to visualize the alternative filter coefficients and how they affect the response. This process is divided to three steps.

In the very first step, possible combination sets are created and compared visually. This part is named as coarse search and worthy of its name, a wide range of the parameters are searched with as few points as possible. Three variables define a three-dimensional space to search. This search step is mostly an engineering judgement part, the range and search points are completely decided based on experiences. Although one may not reach satisfactory sets in the first search due to lack of experience, this part may be repeated many times since it is computationally cheaper with respect to following step. After the ranges and search points are determined, the frequency domain magnitude curves are plotted together with no decoupling case plot. The curves are compared and minimizer candidates are selected.

As an example study, some filter constants and gain values (0.05, 0.8 and 2 rad/s cut-offs for high pass, 3, 5 and 10 rad/s cut-offs for low-pass, and -0.7 to 0.7 linear sweep with a step size of 0.35 for gain) are substituted to one of the feedforward decoupling controller mentioned above. Respective frequency response magnitude curves from longitudinal inputs to lateral autopilot commands are compared. These comparisons can be investigated in Figure 2.

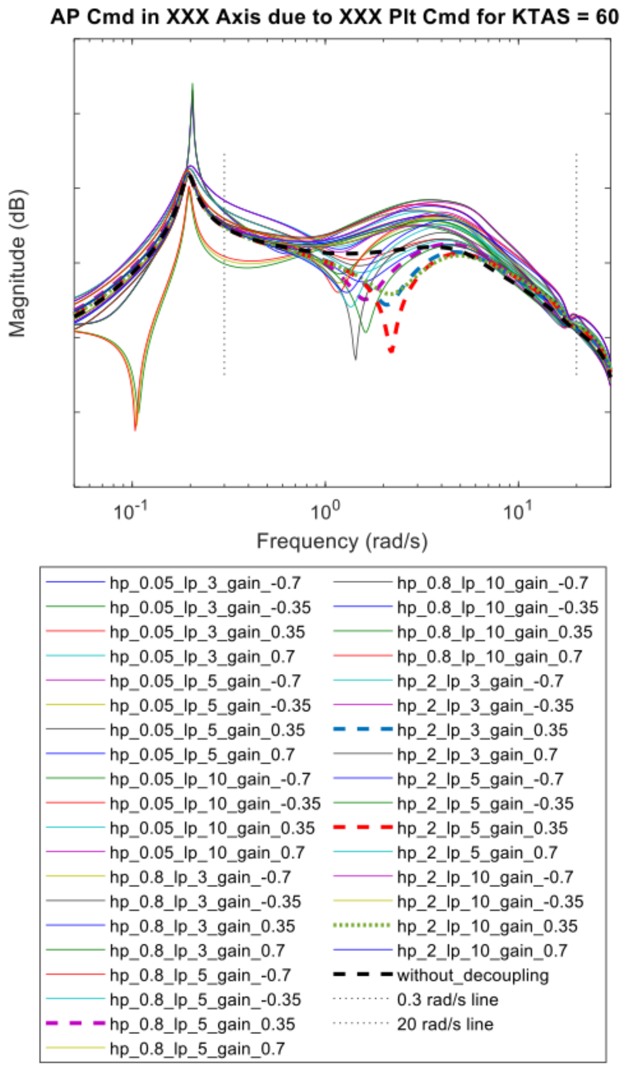

Figure 2. Minimization Process - Coarse Search

Decoupling controller inactive case and all possibilities are compared to select candidates. They are, of course, not required to be best since they will be used to narrow the search area. The candidates are marked by changing their line style to dashed curves after the inspections. In the example, 0.35 gain is common in candidates while 0.8 and 2 rad/s show better results for high pass filter and effect of the low-pass filter coefficient is less significant on the results.

In the second step, the selected minimizer candidates found in the previous step are used to define narrow range of search set. As much number of combinations as possible are aimed to compare in this narrow range. Nevertheless, the same plotting and comparing approach is not efficient in this part, since considering so many plots would be a chaotic process. As a solution, the cost function that best defines the objective has been determined and comparison is done by comparing the cost values. So, an easy to obtain cost function is created like given in equation 1. Also, a saturation is applied to the frequency domain magnitude response difference between with and without decoupling to the equation 4. This saturation is to prevent big differences between these two curves only in a specific frequency range. A predetermined magnitude reduction dB magnitude reduction is enough since it yields a response which is almost insignificant. Greater magnitude reduction is marginal at best for decoupling.

(1) $$J = \sum_{k=1}^{300} \frac{F(j(k\,d\omega + \omega_{\min}))}{1000}$$

(2) $$d\omega = \frac{\omega_{max} - \omega_{min}}{299} = 0.57 \frac{rad}{s}$$

(3) $$\omega_{min} = 0.3, \omega_{max} = 20$$

(4) $$F(\cdot) = \left(\left|H_{dcp}(\cdot)\right| - \left|H_{no\ dcp}(\cdot)\right|\right) \cdot \frac{1}{(\cdot)}$$

The cost function is beneficial since it reduces a frequency domain magnitude curve presentation to a point as measure of reduction. As also stated in the previous step, the tree variables to search defines a 3D space. The resultant cost required to be represented, thus it increases dimension by one to show it on the same plot. To achieve this, for constant high pass filter coefficients, lowpass cut-offs and gain values are used to create x and y axes of a surface plots where z-axis represents the respective costs. The high pass filter coefficients are searched on different plots. 1.1 rad/s and 1.6 rad/s high pass filter coefficient surface plots are shared as examples. Insignificance of lowpass filter coefficients for this search can be seen in the figures.

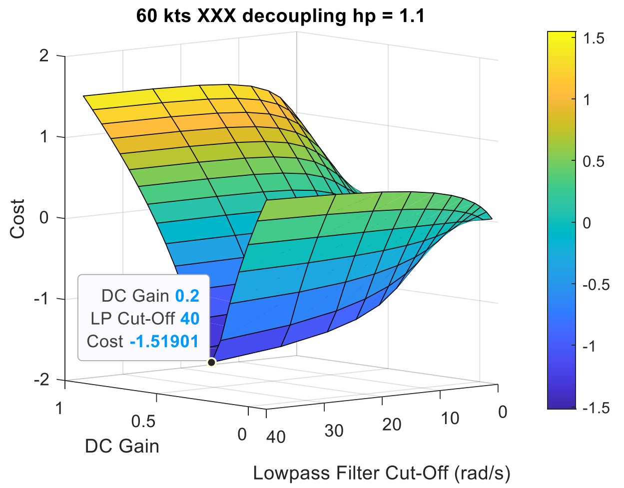

Figure 3. Cost surface plot for highpass filter coefficient of 1.1 rad/s at 60 kts level flight (Decoupling information is concealed.)

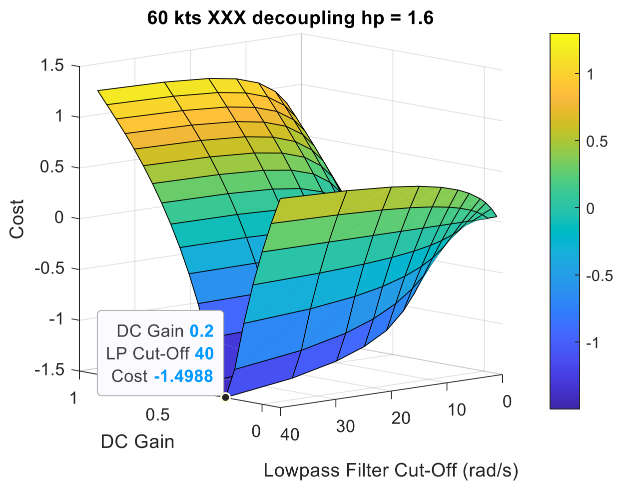

Figure 4. Cost surface plot for highpass filter coefficient of 0.05 rad/s at 60 kts level flight (Axis names are concealed.)

The final step is the comparison step. The first and the second steps mentioned before are repeated for each trim condition in gain scheduling. After the determination of all surface plots for costs, one should find a common filter coefficient set for high pass and lowpass filters. To facilitate the comparison step, trim altitude may be kept constant and only trim speeds may be used in comparisons. The altitude effect on the surface plots is found insignificant (at least in shape) while speed effects are quite important. All possible candidates are selected in this step and compared on frequency domain magnitude plots.

4. DESIGN

In this section, the design steps introduced in section 3 will be applied to inter-axis couplings of T-625 helicopter. Collective to yaw, pitch and roll with pedal to pitch couplings are selected to increase handling qualities of the helicopter as explained in section 2. Collective to yaw decoupling design will be given in details since it is the first one and the procedure is quite same for all, and remaining designs will be explained superficially. Also, collective to pitch decoupling design is emphasized due to its uncommon response characteristics.

4.1. Collective to Yaw Decoupling Design

The design process for collective to yaw decoupling is begun with a coarse search, as previously described. The coarse search part is mostly an engineering judgement part so the intervals for three parameters are defined based on experiences. The results are investigated and coarse search step is repeated to find a better interval. The candidates are selected and given in Figure 5.

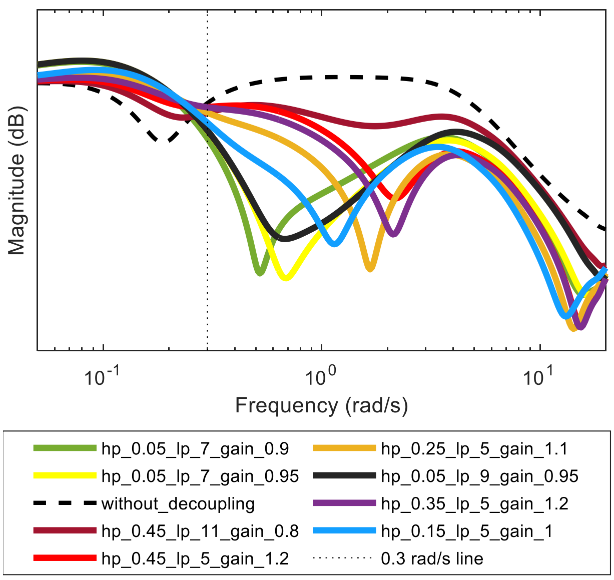

Figure 5. Collective to yaw decoupling coarse search candidates

According to the coarse search study given above, fine search intervals are determined. The cost function given in section 3.3 is used to create surface plots in fine searches. Each surface plot is created for each high pass filter cut-off frequency while gain values and lowpass filter cut-off frequencies are in the abscissa and ordinate axes respectively. One of the surface plots shared in Figure 6 to show shape. Abscissa and ordinate axes rulers are intentionally concealed.

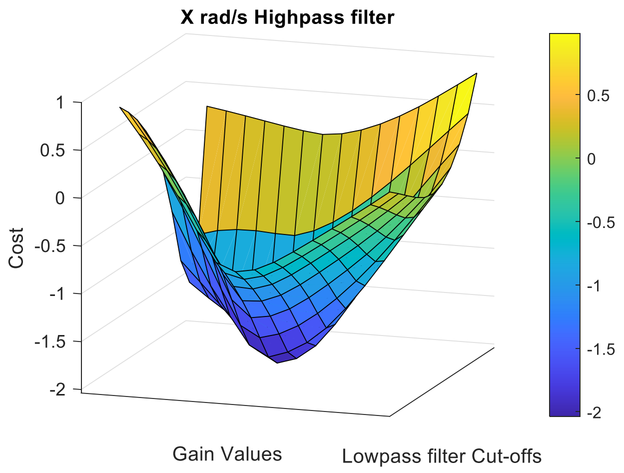

Figure 6. Collective to yaw decoupling fine search for X rad/s highpass filter.

In the bounded discrete domain, defined by the intervals determined in coarse search study, a global minimum point can be seen in Figure 6. Unlike the example given in Figure 3 and Figure 4, lowpass filter cut-off frequency has significant effect on cost. And it should be selected carefully.

Coarse search and fine search studies performed here is done for a certain trim condition and this should be repeated for each trim condition in gain scheduling. This process is resulted in many surfaces. After all those plots are investigated, high pass and lowpass coefficients should be determined to fit best for all trim conditions since they will be constants. On the other hand, gain values are not determined as common constants for selected trim conditions, since they can be scheduled. When the filter coefficient candidates are determined they can be compared on frequency domain plots again. Minimum cost points can be selected from fine search plots for filter coefficient candidates to determine gains in the comparison part. This is to compare filter coefficient candidates with their best possible gain values since gains are schedulable parameters. Comparisons of these candidates are given in Figure 7 and Figure 8. There are only three candidates, because collective to yaw coupling has quite same dynamics in all scheduling trim conditions and this results in close candidates.

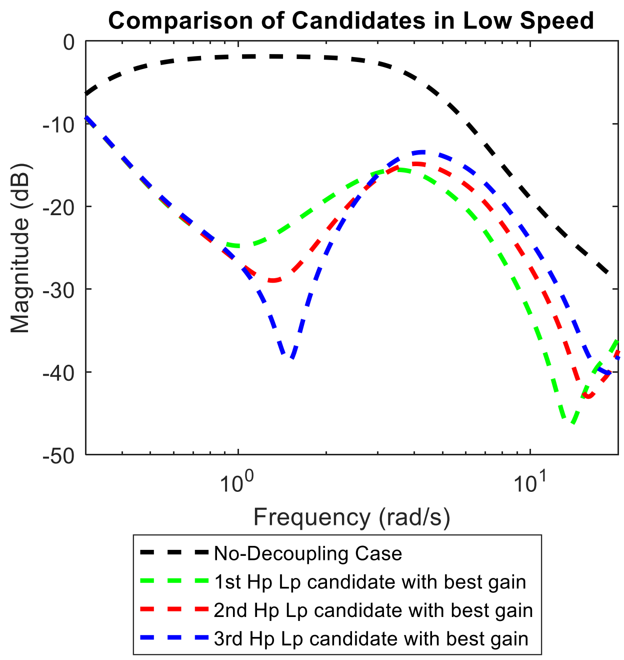

Figure 7. Comparison of three different highpass-lowpass filter coefficient pairs in low speed region.

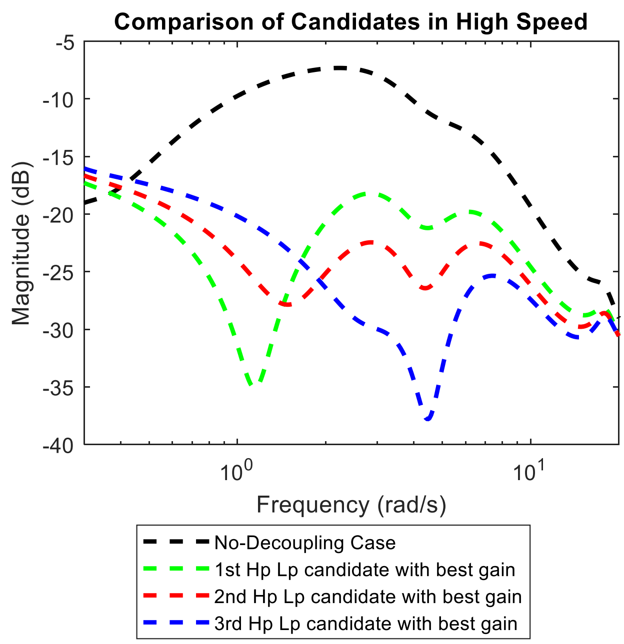

Figure 8. Comparison of three different highpass-lowpass filter coefficient pairs in high speed region.

The red dashed line is selected since it works well in low speed and high speed and also in low frequency region and high frequency region.

After the comparison phase one can also use optimization methods to find gain values without depending on the discretization. However, another approach will be considered here. The helicopter collective to yaw dynamics is expected to change smoothly without any discrete jumps in operating envelope (Ref. 1). This requires to have smooth gain curves. If the gains have unexpected changes, it may be due to discretization or miss-calculations. So, plotting all gains on a figure, and comparing their changes with speed is also a self-control. Resultant gains obtained from the comparison step are transferred to *Figure 9* with pale colors. The broken line appearance is found as due to the discretization of gains in fine search section. Possibility of obtaining smooth lines is compared with the apparent cost function and by re-comparing the results on frequency domain magnitude curves. Although the results didn't show a significant difference on curves, since the change in magnitudes are quite small, it can be said that final smoothed values are better. For the last scheduling speed there are three candidates and their costs are close to each other. This resulted in different choices but the dark color gains are found slightly better.

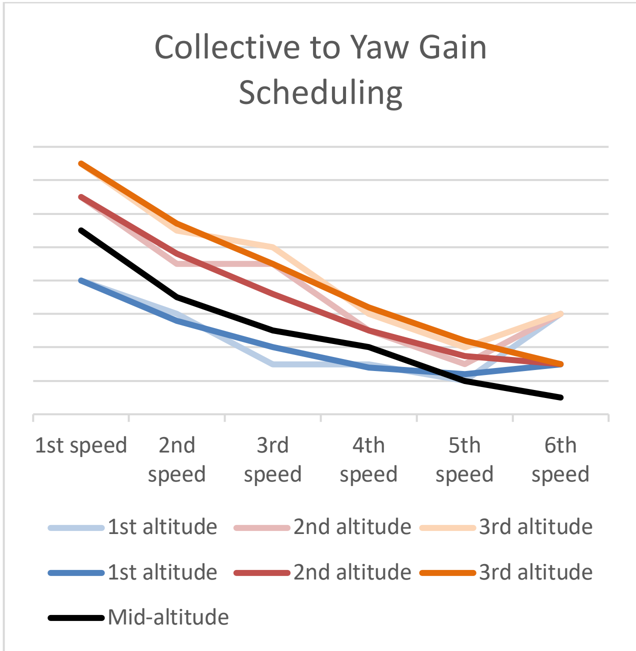

Figure 9. Resultant gains (pale) and smoothed final gains (dark)

4.2. Other Decoupling Designs

Collective to pitch decoupling design process consists of the same steps introduced in section 3.3 and applied to collective to yaw coupling in the previous section. However, an unexpected problem is encountered. Different speeds require gains of different signs. But gain's sign change means the response of the helicopter is changing from one speed to another. For example, in hover the helicopter pitches down with step collective command but in high speed it pitches up. Nevertheless, after investigation of the trim conditions, it is found to be reasonable. In hover and low-speed, the helicopter body pitch angle is the highest, so the center of mass of the body goes forward at most, and the collective response is pitching up. Although this is the case in hover, the response changes to pitching down after 20 kts and goes same after this speed.

This also arises another question regarding how helicopter's collective to pitch response changes with different center of mass locations. This issue was also examined, and it was found that the helicopter's collective to pitch response varied depending on the cg location. But this change does not as big as to require sign change, instead it requires smaller or larger gains to be used and with increasing speeds amount of required change decreases. The gain in first scheduling speed is taken as "0" to not disrupt hover behavior which means the collective to pitch behavior is not changed by the feedforward decoupling control. The gains for second and third scheduling speeds are selected to improve front and aft cg behaviors together. Remaining scheduling speeds are not found to be dependent on cg conditions significantly.

Collective to roll decoupling design steps are also applied in the same order. The expectation was also encountering a cg location dependent coupling since the moment created by the vertical force due to the collective input is also cg dependent. But cg location change envelope in lateral axis is not as large as it was in longitudinal axis and collective to roll dynamics is affected by the helicopter main regressive rotor flapping and fuselage roll mode coupling mostly (Ref. 1) Although detailed investigation of helicopter dynamics is out of scope of this study, one can continue with the information regarding this resulted in negligible cg effects in operating envelope of the helicopter.

Pedal to pitch decoupling is the last part of this section. Importance of this decoupling comes from the cant angle of T-625 GÖKBEY helicopter. Also feedforward collective to yaw decoupling design creates pedal command due to collective inputs. It also resulted in pitch response when a collective input applied by the pilot due to aforementioned cant angle. Feedforward pedal to pitch decoupling is also designed by following the same procedure. The results will be investigated in next sections.

5. SIMULATOR AND FLIGHT TESTS

After the design is complete, the designed decoupling controllers are tested in simulator and flight tests. First, the methodology of the tests will be explained.

5.1. Test Methodology

Tests are planned to cover performance checks on all scheduling points, both airspeeds and altitudes. Tests contain two different methodologies, time domain and frequency domain testing.

Time domain tests introduce collective step in-puts given by the pilot. The pilot is asked to trim the helicopter at desired altitude and airspeed and hold the trim for 5 seconds to account for withdrawal of decoupling commands from previous inputs. Then, the pilot is asked to give 10% collective step input. To show symmetry, pilot is asked to give up step and down step inputs. After the input is introduced, pilot is asked to not give any commands in any other axes. After approximately 3 seconds, commands generated by ATT controller become more dominant than decoupling controller as the effect of the pilot input is fading away. The goal is to investigate off-axis responses of the helicopter. The generated rates, angles and actuator commands are compared for decoupling controller active and inactive cases. Together with data, pilot commands are also distinctive in time-domain tests as the pilots can clearly distinguish the effect of decoupling controller.

Frequency domain tests introduce collective sweep input given by the pilot. After the desired trim is achieved, pilot is asked to maintain the trim for 5 seconds to account for withdrawal of decoupling commands from previous inputs. Then, the pilot is asked to excite the collective stick giving sinusoidal inputs changing frequency in the frequency range of interest. Then, the off-axis autopilot generated commands are observed. In sweep excitation, it is hard for the pilots to give any performance judgement, so their comments are not as distinctive as in time domain tests. For decoupling controller active case, decoupling commands are subtracted from total autopilot commands. The frequency response function magnitude curve from pilot collective command to off-axis autopilot command is generated for all axes and the differences between decoupling active and inactive cases are highlighted. It should be noted that this test method is not definitive as the coherence between off-axis autopilot command and pilot collective command will likely be low. This suggests that any conclusion drawn from frequency response function has questionable reliability. However, the authors believe that it can give some idea to helicopter coupling behavior at different frequencies. This thought is built upon the usage in ADS-33E-PRF (Ref. 4) of rate to off-axis rate frequency response function magnitude average to judge decoupling performance. Tischler et. al. (Ref.3) utilized command to off-axis rate and command to on-axis rate frequency response magnitude curves to build the aforementioned relationship, as given in Section 3.1. Thus, command to off-axis rate frequency response carries valuable information regarding helicopter coupling behavior.

5.2. Simulation Tests

In simulator environment, time domain oriented collective step tests are performed. The frequency domain sweep tests are not carried out because the model in simulator environment was already known and the test results would be parallel to desktop simulations. Additionally, pilot comments in between test points are taken to understand their perspective on the change in helicopter behavior during normal operation. An example result is given in Figure 10. The results illustrate off-axis rate responses to 13% collective stick command. Rate responses are chosen for illustration as they are a clear indication of SAS autopilot command. The designed decoupling controller minimizes the generated off-axis rate. This is achieved thanks to the feedforward structure choice, as the necessary command to counteract the coupling effect is generated much faster. It can also be seen that after 19th second, ATT performance becomes more dominant than decoupling performance. This is evident as rate outputs reach their steady state values for both decoupling active and inactive cases after 19th second. Pilot comments are supporting the test results, the helicopter behavior is much more decoupled.

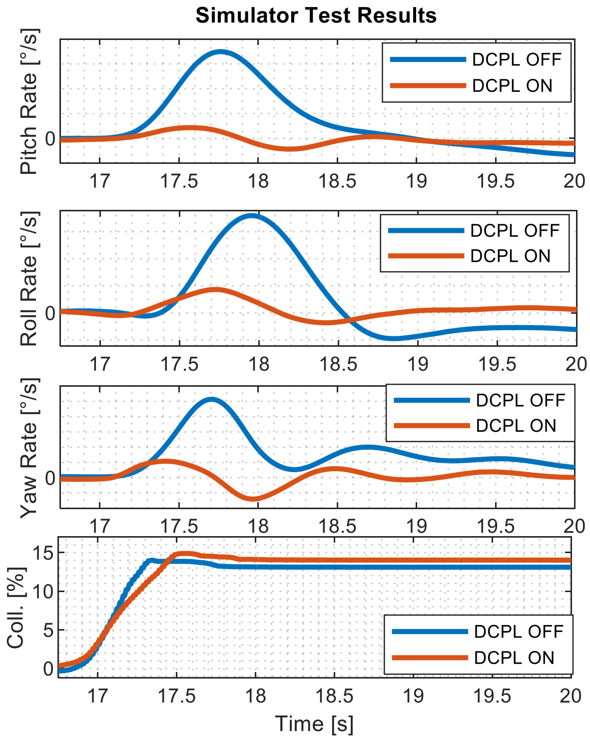

Figure 10. Simulator Test Example Results

5.3. Flight Tests

In flight tests, both time domain and frequency domain tests are carried out. Unlike the simulator environment, this time, the actual helicopter flight dynamics are in effect and model uncertainties must be accounted for. Again, pilot perspective in between test points is taken. An example for time domain flight test is given in Figure 11 and one ex-ample for frequency domain flight test is given in Figure 12.

In Figure 11, off-axis rate responses to 15% down step collective input are given. Rate responses are significantly less for decoupling active cases. The time domain flight test results are matching the outcomes of the simulator tests.

In Figure 12, frequency domain magnitude plots are shared together with coherence values in each axis. In all axes, response magnitude is less for decoupling active cases in the majority of the frequency range. The regions where decoupling on cases has larger response magnitude then decoupling off cases has a coherence value less than 0.6 (Ref 10), the acceptable limit for reliable comparison. One other point to highlight is the drop of coherence values. For all axes, mean coherence value is less for de-coupling active cases. This shows that the input and output signals are less correlated, more decoupled. This side result can also be treated as a supporting outcome.

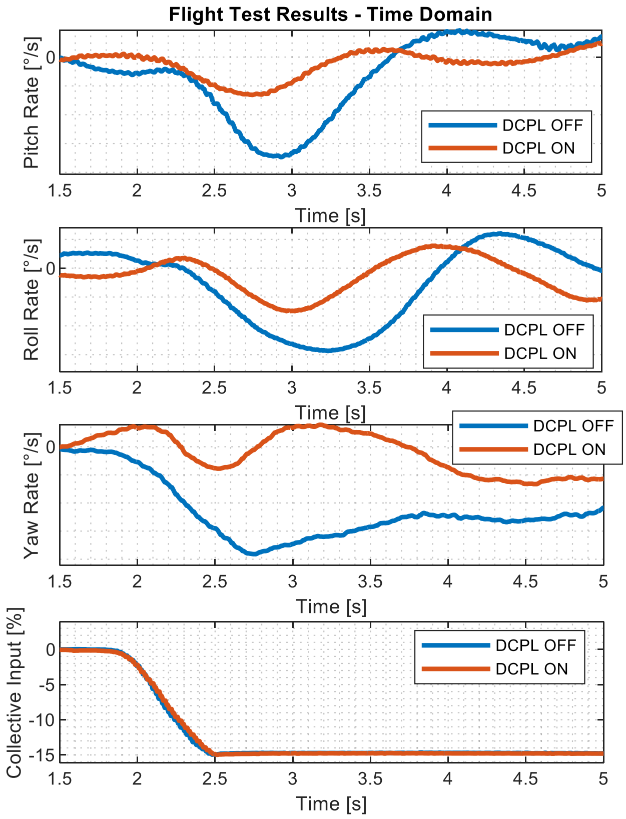

Figure 11. Flight Test Example Results - Time Domain

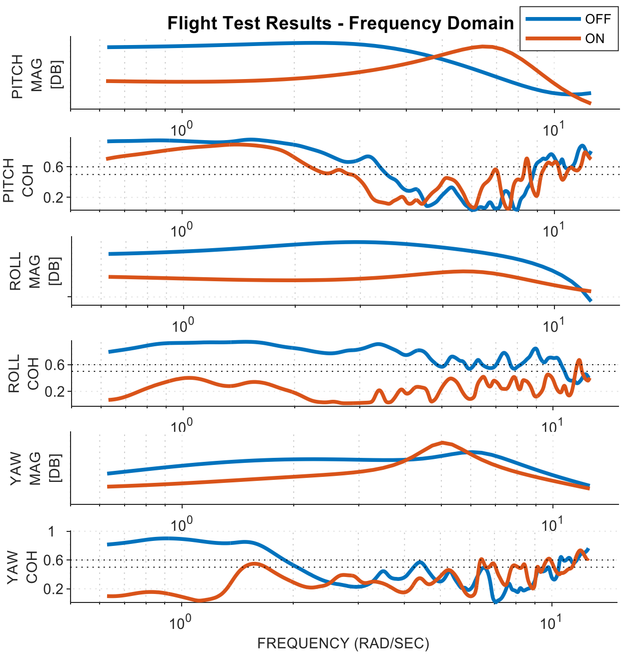

Figure 12. Flight Test Example Results - Frequency Domain

6. CONCLUSIONS

The important realizations of this study can be summarized as follows:

1. A feedforward decoupling controller is designed using a lowpass, high pass and a DC gain.
2. The design parameters are optimized investigating on-axis rate response to off-axis rate response and on-axis pilot command to off-axis autopilot command input-output pairs.
3. Filter cut-offs and DC gains are optimized through the utilization of a cost function that qualitatively defines magnitude differences between coupled and decoupled frequency response magnitude curves in the frequency range of interest, which covers pilot commands given under normal conditions.
4. Filter cut-offs are held constant but DC gain is scheduled for different airspeed and altitude scheduling points.
5. This process is repeated for collective to yaw, pitch and roll couplings and yaw to pitch coupling.
6. Designed controllers are tested in simulator and flight tests through time domain collective step inputs and frequency sweep inputs. The results show decreased coupling characteristics and the success of the design.

As a note to vertical flight researchers, the authors would like to highlight the absence of clear decoupling requirements for rotorcraft controller design. This study was conducted due to a lack of common decoupling requirements in helicopter industry. The helicopter industry needs a solid and understandable way to design decoupling controllers. The authors hope that studies like this will be a call to action to all vertical flight society to work on establishing common decoupling requirements.

Author contact:

Oğuzhan Gültekin oguzhan.gultekin@tai.com.tr

Can Ünen can.unen2@tai.com.tr

Umut Türe umut.ture@tai.com.tr

Ilgaz Doğa Okcu iokcu@tai.com.tr

7. REFERENCES

1. Padfield, G., *Helicopter Flight Dynamics: including a treatment of tiltrotor aircraft*, John Wiley & Sons, Hoboken, NJ, 2018, Chapter 6.

2. Zhang, M. and Ma, J., "Dual-loop hovering control for unmanned helicopter," *Journal of Physics Conference Series*, Vol. 2224(1), 2022. DOI: 10.1088/1742-6596/2224/1/012106

3. Tischler, M. B., Berger, T., Ivler, C. M., Mansur, M. H., Cheung, K. K., Soong, J. Y., *Practical Methods for Aircraft and Rotorcraft Flight Control Design: An Optimization-Based Approach,* AIAA Education Series, Reston, VA, 2017, Chapter 5

4. Anon., "Aeronautical Design Standard, Handling Qualities Design Requirements for Military Rotorcraft," USAAMCOM ADS-33E-PRF, 2000.

5. Catapang, D. R., Tischler, M. B., Biezad, D. J., "Robust Crossfeed Design for Hovering Rotorcraft", *International Journal of Robust and Nonlinear Control*, Vol. 4(1), 1994, pp. 161-180.

6. Lu, G., "Aggressive attitude control of unmanned rotor helicopters using a robust controller," *Journal of Intelligent & Robotic Systems*, Vol. 80(1), 2014, pp: 165-180. DOI: 10.1007/s10846-014-0160-4

7. Tian, S., Wang, J., Lin, D., & Pei, P., " l1 adaptive control design of a helicopter in vertical flight," *Proceedings of the Institution of Mechanical Engineers Part G Journal of Aerospace Engineering*, Vol. 234(14), pp: 2089-2099. DOI:10.1177/0954410020926619

8. Goodwin, G. C., Graebe, S. F., Salgado, M. E., *Control System Design,* Prentice Hall, Hoboken, NJ, 2001, Chapter 26.

9. Hui, L. C., *Lecture Notes in Control and Information Sciences: General Decoupling Theory of Multivariable Control Systems,* Springer-Verlag, Berlin, 1983, Chapter 4.

10. Tischler, M.B., Remple, R. K., *Aircraft and Rotorcraft System Identification: Engineering Methods with Flight Test Examples*, AIAA Education Series, Reston, VA, 2006, Chapter 7

8. CLASSIFICATION & COPYRIGHT